

**Special Issue: Manufacturing of Advanced
Biodegradable Polymeric Components**

Guest Editors: Prof. Roberto Pantani (University of Salerno) and
Prof. Lih-Sheng Turng (University of Wisconsin-Madison)

EDITORIAL

Manufacturing of advanced biodegradable polymeric components

R. Pantani and L.-S. Turng, *J. Appl. Polym. Sci.* 2015, DOI: [10.1002/app.42889](https://doi.org/10.1002/app.42889)

REVIEWS

Heat resistance of new biobased polymeric materials, focusing on starch, cellulose, PLA, and PHA

N. Peelman, P. Ragaert, K. Ragaert, B. De Meulenaer, F. Devlieghere and Ludwig Cardon, *J. Appl. Polym. Sci.* 2015, DOI: [10.1002/app.42305](https://doi.org/10.1002/app.42305)

Recent advances and migration issues in biodegradable polymers from renewable sources for food packaging

P. Scarfato, L. Di Maio and L. Incarnato, *J. Appl. Polym. Sci.* 2015, DOI: [10.1002/app.42597](https://doi.org/10.1002/app.42597)

3D bioprinting of photocrosslinkable hydrogel constructs

R. F. Pereira and P. J. Bartolo, *J. Appl. Polym. Sci.* 2015, DOI: [10.1002/app.42458](https://doi.org/10.1002/app.42458)

ARTICLES

Largely toughening biodegradable poly(lactic acid)/thermoplastic polyurethane blends by adding MDI

F. Zhao, H.-X. Huang and S.-D. Zhang, *J. Appl. Polym. Sci.* 2015, DOI: [10.1002/app.42511](https://doi.org/10.1002/app.42511)

Solubility factors as screening tools of biodegradable toughening agents of polylactide

A. Ruellan, A. Guinault, C. Sollogoub, V. Ducruet and S. Domenek, *J. Appl. Polym. Sci.* 2015, DOI: [10.1002/app.42476](https://doi.org/10.1002/app.42476)

Current progress in the production of PLA-ZnO nanocomposites: Beneficial effects of chain extender addition on key properties

M. Murariu, Y. Paint, O. Murariu, J.-M. Raquez, L. Bonnaud and P. Dubois, *J. Appl. Polym. Sci.* 2015, DOI: [10.1002/app.42480](https://doi.org/10.1002/app.42480)

Oriented polyvinyl alcohol films using short cellulose nanofibrils as a reinforcement

J. Peng, T. Ellingham, R. Sabo, C. M. Clemons and L.-S. Turng, *J. Appl. Polym. Sci.* 2015, DOI: [10.1002/app.42283](https://doi.org/10.1002/app.42283)

Biorenewable polymer composites from tall oil-based polyamide and lignin-cellulose fiber

K. Liu, S. A. Madbouly, J. A. Schrader, M. R. Kessler, D. Grewell and W. R. Graves, *J. Appl. Polym. Sci.* 2015, DOI: [10.1002/app.42592](https://doi.org/10.1002/app.42592)

Dual effect of chemical modification and polymer precoating of flax fibers on the properties of the short flax fiber/poly(lactic acid) composites

M. Kodal, Z. D. Topuk and G. Ozkoc, *J. Appl. Polym. Sci.* 2015, DOI: [10.1002/app.42564](https://doi.org/10.1002/app.42564)

Effect of processing techniques on the 3D microstructure of poly(L-lactic acid) scaffolds reinforced with wool keratin from different sources

D. Puglia, R. Ceccolini, E. Fortunati, I. Armentano, F. Morena, S. Martino, A. Aluigi, L. Torre and J. M. Kenny, *J. Appl. Polym. Sci.* 2015, DOI: [10.1002/app.42890](https://doi.org/10.1002/app.42890)

Batch foaming poly(vinyl alcohol)/microfibrillated cellulose composites with CO₂ and water as co-blowing agents

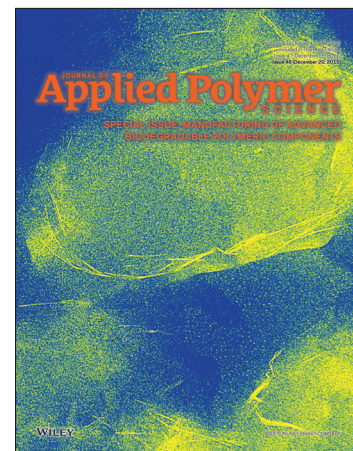
N. Zhao, C. Zhu, L. H. Mark, C. B. Park and Q. Li, *J. Appl. Polym. Sci.* 2015, DOI: [10.1002/app.42551](https://doi.org/10.1002/app.42551)

Foaming behavior of biobased blends based on thermoplastic gelatin and poly(butylene succinate)

M. Oliviero, L. Sorrentino, L. Caferio, B. Galzerano, A. Sorrentino and S. Iannace, *J. Appl. Polym. Sci.* 2015, DOI: [10.1002/app.42704](https://doi.org/10.1002/app.42704)

Reactive extrusion effects on rheological and mechanical properties of poly(lactic acid)/poly[(butylene succinate)-co-adipate]/epoxy chain extender blends and clay nanocomposites

A. Mirzadeh, H. Ghasemi, F. Mahrous and M. R. Kamal, *J. Appl. Polym. Sci.* 2015, DOI: [10.1002/app.42664](https://doi.org/10.1002/app.42664)



**Special Issue: Manufacturing of Advanced
Biodegradable Polymeric Components**

Guest Editors: Prof. Roberto Pantani (University of Salerno) and
Prof. Lih-Sheng Turng (University of Wisconsin-Madison)

Rotational molding of biodegradable composites obtained with PLA reinforced by the wooden backbone of opuntia ficus indica cladodes

A. Greco and A. Maffezzoli, *J. Appl. Polym. Sci.* 2015, DOI: [10.1002/app.42447](https://doi.org/10.1002/app.42447)

Foam injection molding of poly(lactic) acid: Effect of back pressure on morphology and mechanical properties

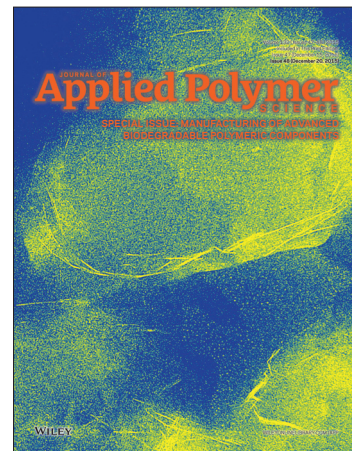
V. Volpe and R. Pantani, *J. Appl. Polym. Sci.* 2015, DOI: [10.1002/app.42612](https://doi.org/10.1002/app.42612)

Modification and extrusion coating of polylactic acid films

H.-Y. Cheng, Y.-J. Yang, S.-C. Li, J.-Y. Hong and G.-W. Jang, *J. Appl. Polym. Sci.* 2015, DOI: [10.1002/app.42472](https://doi.org/10.1002/app.42472)

Processing and properties of biodegradable compounds based on aliphatic polyesters

M. R. Nobile, P. Cerruti, M. Malinconico and R. Pantani, *J. Appl. Polym. Sci.* 2015, DOI: [10.1002/app.42481](https://doi.org/10.1002/app.42481)



Current progress in the production of PLA-ZnO nanocomposites: Beneficial effects of chain extender addition on key properties

Marius Murariu, Yoann Paint, Oltea Murariu, Jean-Marie Raquez, Leila Bonnaud, Philippe Dubois

Center of Innovation and Research in Materials and Polymers (CIRMAP), Laboratory of Polymeric and Composite Materials (LPCM), University of Mons & Materia Nova Research Center, Place du Parc 20, 7000, Mons, Belgium

Correspondence to: M. Murariu (E-mail: marius.murariu@materianova.be) and P. Dubois (E-mail: philippe.dubois@umons.ac.be)

ABSTRACT: Poly(lactic acid) (PLA) nanocomposites characterized by multifunctional end-use properties are of high interest as new biosourced materials for the production of smart films, fibers, and injection-molded components. In this work, PLA-ZnO nanocomposites designed for the extrusion of films were obtained by melt-compounding PLA with up to 5 wt % ZnO rod-like nanoparticles, nanofiller previously surface-treated with a specific silane (triethoxycaprylylsilane). To improve the processing and performances of nanocomposites such as their stability at high temperature, the addition of a selected chain-extender (CE) was considered. It was revealed that the co-addition of nanofiller (ZnO) and epoxy functional styrene-acrylate oligomeric CE (Joncryl[®] ADR 4300F) leads to a very significant enhancement of the properties (molecular, rheological, thermal, etc.) of PLA-ZnO nanocomposites. After addition of 1% CE into nanocomposites, the PLA molecular weights were found to be nearly twofold higher, while the isothermal tests (at 220 and 240°C) confirmed a significant increase in thermal stability. Because the CE plays a key role in limiting the degrading effects of ZnO, due to a gain in melt viscosity and increased molecular mass, a better ability to process nanocomposites by extrusion was found. The good nanofiller dispersion and specific end-use characteristics owing to the presence of ZnO nanoparticles (such as UV shielding) were again confirmed on extruded films. These developments are being viewed as a promising approach that can open new perspectives in the application of PLA-ZnO nanocomposites with specific end-use properties (UV protection, antibacterial, gas-barrier, and self-cleaning) at larger scale. © 2015 Wiley Periodicals, Inc. *J. Appl. Polym. Sci.* **2015**, *132*, 42480.

KEYWORDS: biopolymers and renewable polymers; degradation; extrusion; films; nanoparticles

Received 1 February 2015; accepted 5 May 2015

DOI: 10.1002/app.42480

INTRODUCTION

The extraordinary interest and growth in the global production of biopolymers is connected to a big number of factors including consumer demand for more environmentally sustainable products, the development of bio-based feed-stocks, increase of restrictions for the use of polymers with high “carbon footprint” of petrochemical origin, particularly in such applications as packaging, automotive, electrical and electronics industry, and so on.^{1–6}

In competition with petroleum-based polymers, poly(lactic acid) or polylactide (PLA) is one of the most promising candidates for future developments; it not only is (bio)degradable under controlled composting conditions, but also produced from renewable natural resources by fermentation of polysaccharides or sugar, e.g., extracted from corn or sugar beet, and corresponding wastes.^{3,7–10}

PLA is currently receiving a considerable attention for traditional applications such as packaging, as well as production of textile fibers, and interestingly enough, it also finds higher added value for technical applications.^{6,11–13} Nowadays, the addition into PLA of selected nanofillers (e.g., organomodified layered silicates (OMLS), silver, zinc oxide, graphite derivatives, carbon nanotubes (CNT), silica, etc.) is considered as a modern approach that can lead to major improvements of PLA characteristic features (mechanical, thermal, barrier, etc.). Furthermore, these nanocomposites are characterized by specific end-use properties such as anti-UV and anti-bacterial, antistatic to conductive electrical characteristics, enhanced wear resistance, higher crystallization speed, and fire retardancy.^{1,5,8,14–21}

Zinc oxide (ZnO) is a well-known environmentally friendly and multifunctional inorganic nanofiller, with an optical band gap in the UV region that makes it useful as an efficient UV-light absorber. ZnO nanofillers can be mixed with different polymers

Additional Supporting Information may be found in the online version of this article.

© 2015 Wiley Periodicals, Inc.

(polyamide 6, epoxy and acrylic resins, poly(methyl methacrylate), polystyrene, polypropylene, etc.) to produce nanocomposites characterized by a large array of properties such as effective antibacterial protection, intensive ultraviolet absorption, or other characteristic features.^{22–24}

Interestingly, ZnO nanoparticles and Zn derivatives are known as very efficient catalysts in the synthesis of PLA through ring-opening polymerization of lactide as well as in “unzipping” depolymerization of PLA.^{25,26} Indeed, some of us have reported that the addition of untreated ZnO nanoparticles into PLA at melt-processing or at higher temperature led to the severe degradation of the polyester matrix.²⁷ However, by considering the high propensity of Zn-based products (such as untreated ZnO) to trigger PLA degradation, other researchers have preferred to use the solvent casting method for the production of PLA–ZnO nanocomposites.¹⁸ On the other hand, following the surface treatment of ZnO nanoparticles with specific silanes, it was reported by us the possibility to produce PLA-based nanocomposites via melt-compounding in internal mixers or using twin-screw extruders, an approach which is creating new opportunities for their application at larger scale.^{27–29} These nanocomposites at various loading of nanofiller have been tested in the production of fibers, films, or other materials, showing multifunctional end-use properties (anti-UV, antibacterial, barrier, etc.).^{27,28} In our opinion, the melt-blending manufacturing method has larger applicability with respect to other techniques, such as the solvent casting.

It is also worth recalling that PLA is very sensitive to temperature, shear, and hydrolysis during melt-processing. To overcome the results of PLA degradation (during production and processing), like other condensation polymers (polyethylene terephthalate, polyamides, polycarbonates, etc.),³⁰ the addition of multifunctional chain extenders (CE) into PLA is seen as an attractive low-cost method which could counterbalance the molecular weight degradation. However, among the CEs recently reported for PLA (polycarbodiimide (PCDI),³¹ tris(nonylphenyl) phosphite (TNPP),³² diisocyanate derivatives,³³ etc.), it is worth pointing out the utilization of styrene-acrylic multifunctional-epoxide oligomeric CEs such as Joncryl[®] products. These additives are commercialized with different characteristic features (glass transition temperature, molecular weight, epoxide concentration, etc.). They possess epoxy groups as primary reactive functionalities, which preferentially react with PLA end groups to generate esters or ethers of increased weight-average molecular weight and viscosity.^{34–40}

PLA end groups (i.e., carboxylic acid and hydroxyl end-groups), which are additionally formed due to thermal and oxidative degradation or especially when PLA is heated in the presence of water, can react with epoxy functional groups creating covalent bonds.^{40–42} These additives are also considered as good compatibilizers for the production of PLA-based blends. They are also of high effectiveness in the increasing of PLA hydrolytic stability and melt strength, processing output, etc., all at very low loading levels.⁴³

Besides, in many cases, the mixing of PLA with additives and nanofillers is followed by the important drop of molecular

weights, together with the loss of thermal, rheological, and mechanical properties. However, it is often stated out in literature that addition of nanofillers (e.g., OMLS) into PLA can intensify its rate of degradation and molecular weight reduction. To limit the degrading effect of OMLS, Najafi *et al.* have studied the effects of incorporation of CEs (from the category of multifunctional-epoxide oligomers) into PLA nanocomposites. It was reported that addition of CE at an appropriate loading had a profound effect not only on the control of polymer degradation but also on the increase of molecular weights and consequently, on the polymer viscosity.^{37,38}

Regarding the utilization of ZnO as nanofiller for PLA, it is noteworthy mentioning that the silanization of nanoparticles is a prerequisite to limit the degradation of the polyester matrix. Furthermore, the extent of thermal degradation of PLA increases in direct correlation to ZnO loading.²⁷ Unfortunately, in the real case of industrial applications and especially at high processing temperature and/or long residence time, these nanocomposites do not show the advanced stability that can be required by end users to produce films, fibers, injection molded parts, etc., since the decrease of molecular parameters strongly affects their thermal, melt-fluidity, and mechanical properties. Therefore, the control of thermal degradation of these nanocomposites represents a major challenge and this study is an answer to this demand.

In this work, tailored epoxy-functional styrene-acrylic oligomers have been evaluated as CEs to improve the properties (molecular, thermal, rheological, etc.) of PLA–ZnO nanocomposites while maintaining their specific end-use characteristics. PLA–ZnO nanocomposites (with or without CE) were produced by melt-compounding using twin-screw extruders, step followed by their processing by extrusion as films. Furthermore, the comparative evaluation of properties has been performed to highlight the improvements in the performances of so-produced nanocomposites, their specific end-use characteristics and to attire the interest for a potential application at larger scale.

EXPERIMENTAL

Materials

Poly(L,L-lactide)—hereafter called PLA—supplier NatureWorks LLC, was a grade designed for the extrusion of films (4032D) with $M_n = 133,000$, dispersity (D), $M_w/M_n = 1.94$ (M_w and M_n being, respectively, weight- and number-average molar mass expressed in polystyrene equivalent), whereas according to the producer, the other characteristics are as follows: D isomer = 1.4%; relative viscosity = 3.94; and residual monomer = 0.14%.

Silane-treated ZnO nanofiller was supplied by Umicore Zinc Chemicals (Belgium) as Zano 20 Plus (surface treated with triethoxycaprylsilane, ZnO content about 96%). According to supplier and our transmission electron microscopy (TEM) investigation, these nanoparticles are characterized by a rod-like morphology, having diameters of 15–30 nm and a maximum length of 100 nm.²⁸

Joncryl[®] ADR-4300F was kindly supplied by BASF and used here as PLA chain extender with mild-epoxy functionality.

Table I. Composition and Codification of PLA Nanocomposite Samples Considered in This Study

Entry	Sample code	Composition (wt %)		
		PLA	ZnO	CE
1	1ZnO	99	1	-
2	1ZnO/0.5J	98.5	1	0.5
3	1ZnO/1J	98	1	1
4	3ZnO	97	3	-
5	3ZnO/0.5J	96.5	3	0.5
6	3ZnO/1J	96	3	1
7	5ZnO	95	5	-
8	5ZnO/0.5J	94.5	5	0.5
9	5ZnO/1J	94	5	1

According to the technical sheet, this product (supplied in flakes form) has $M_w = 5500$, epoxy-equivalent by weight 445 g/mol and a glass transition temperature of about 56°C.⁴⁴ It will be mentioned hereinafter as “Joncryl” or it will be abbreviated as “CE”.

Ultranox 626A (Bis (2,4-di-*t*-butylphenyl) Pentaerythritol Diphosphite) supplied by Brenntag NV (called below as U626) was selected as thermal stabilizer and used at a preferred percentage of 0.3 wt % in all PLA compositions. Throughout this contribution, all percentages are given as weight percent (wt %).

Preparation of Nanocomposites

Before processing, PLA was dried at 70°C overnight using a drying oven with recirculating hot air. To minimize the water content for melt-blending with PLA, the ZnO nanofiller was previously dried using similar conditions. PLA granules were dry-mixed with the nanofiller and additives (CE and U626) using a Zeppelin Henschel intensive mixer. Then, PLA nanocomposites (with 1, 3, and 5% ZnO) and having up to 1% CE were prepared by melt-compounding using a twin-screw extruder Leistritz ZSE 18 HP-40D (screw diameter (D) = 18 mm, L (length)/ D ratio = 40) and the following processing conditions: throughput of 2 kg/h, screw speed = 150 rpm, temperatures of extrusion on the heating zones adapted to the rheological characteristics of PLA blends (e.g., extrusion temperatures on heating zones: Z1 = 185°C; Z2 = 195°C; Z3 = 205°C; Z4–Z6 = 200°C; Z7 = 195°C in the case of nanocomposites with CE), while the temperature of the molten polymer before the extrusion of strands was kept around 195°C. For the sake of comparison, PLA–ZnO nanocomposites without CE were produced under similar melt-compounding conditions, except that the extrusion temperatures which were with about 10°C lower than in the case of the blends containing CE. The composition and codification of nanocomposite samples produced by melt-compounding is shown in Table I.

Then, the previously dried pellets (drying under vacuum at 70°C overnight) from selected nanocomposites were extruded as films of 100 and 300 μm thickness with a Brabender single-

screw extruder ($D = 19$ mm, $L/D = 25$) adapted with a extrusion die head (ribbon die of 100 mm wide, gap of 0.5 mm) and using for drawing a Univex flat film take-off with the nip rolls heated at about 60°C as downstream equipment.

Characterization

Size Exclusion Chromatography. Molecular weight determination of PLA was carried out on samples dissolved in chloroform (10 mg polymer/5 mL solvent). Size exclusion chromatography (SEC) measurements on previous filtered samples were performed at 30°C using an Agilent liquid chromatograph equipped with an Agilent degasser, an isocratic HPLC pump (flow rate = 1 mL/min), an Agilent autosampler (loop volume = 100 μL), an Agilent-DRI refractive index detector and three columns: a PL gel 5 μm guard column and two PL gel Mixed-B 5 μm columns (linear columns for separation of molecular weights (PS standards) ranging from 200 to 4×10^5 g/mol). The experimental errors in the case of SEC measurements are estimated to be about 10%. Molecular weights and molecular distributions were calculated by reference to a universal calibration curve relative to polystyrene standards.

Thermogravimetric Analysis. Thermogravimetric analysis (TGA) was performed by using a TGA Q50 (TA Instruments) at a heating ramp of 20°C/min under air flow, from room temperature up to 600°C (platinum pan, 60 cm^3/min air flow rate). Isothermal tests as simulated by TGA were performed by using HiRes TGA 2950 (TA Instruments) (platinum pans, air flow rate of 110 cm^3/min). Procedure: heating ramp of 20°C/min from room temperature up to the desired temperature (e.g., 220 or 240°C), followed by an isotherm for up to 60 min.

Differential Scanning Calorimetry. Differential scanning calorimetry (DSC) measurements were performed by using a DSC Q200 from TA Instruments under nitrogen flow. The procedure was as follows: first heating scan at 10°C/min from 0°C up to 200°C, isotherm at this temperature for 2 min, then cooling down at 10°C/min to -20°C and finally, second heating scan from -20 to 200°C at 10°C/min. The first scan was used to erase the prior thermal history of the samples. The events of interest, i.e., the glass transition temperature (T_g), cold crystallization temperature (T_c), enthalpy of cold crystallization (ΔH_c), melting temperature (T_m), and melting enthalpy (ΔH_m) were typically determined from the second scan. Noteworthy, for all samples, only the fraction of PLA was considered. The degree of crystallinity was determined by subtracting ΔH_c from ΔH_m and by considering a melting enthalpy of 93 J/g for 100% crystalline PLA.

Rheological Measurements. The melt flow index (MFI) of selected samples was determined using an automatic Davenport 10 melt flow indexer and the measurements were performed at the temperature of 190°C following the procedure described in ASTM D1238 (standard die 2.095×8 mm and using a 2.16 kg load).

To get information about the behavior of nanocomposites in the molten state at selected temperatures, a rheometer ARES-LS (TA Instruments) equipped with 25 mm parallel plates was used for rheological measurements. The testing was conducted

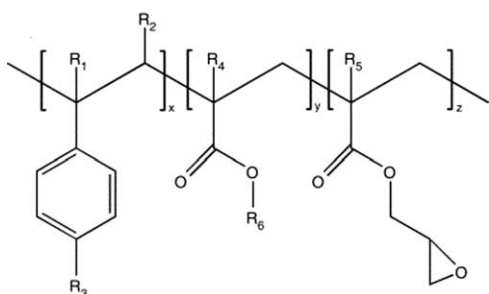


Figure 1. General structure of the styrene-acrylic multifunctional epoxy oligomeric chain extenders. Where R_1 – R_5 are H, CH_3 , a higher alkyl group, or combinations of them; R_6 is an alkyl group, and x , y , and z are each between 1 and 20. Reprinted with Elsevier permission from the reference Villalobos *et al.*³⁰

on previously dried samples under controlled deformation conditions: gap of 1.2 mm, strain = 10%, the dynamic frequency sweeps were carried out over an angular frequency range of 0.01 up to 700 rad/s.

Mechanical Testing. Tensile testing measurements were performed on dog-bone specimens (type V, ASTM D 638-02a) obtained by cutting from the extruded films (100 μm thickness) using a Lloyd LR 10K tensile bench at a tensile rate of 1 mm/min, with a distance of 25.4 mm between grips. All mechanical tests were carried out by using specimens previously conditioned for at least 48 h at $20 \pm 2^\circ\text{C}$ under a relative humidity of $50 \pm 3\%$ and the values were averaged out over minimum five measurements.

Transmission Electron Microscopy. Transmission electron micrographs were obtained with a Philips CM200 apparatus using an accelerator voltage of up to 120 kV. The samples (70–80 nm thick) were prepared with a Leica Ultracut UCT ultramicrotome by cutting them at -100°C . Reported microphotographs represent typical morphologies as observed at, at least, three different locations.

UV Absorption Properties. UV-visible absorption spectra were measured on films of about 100 μm thickness using an UV-vis Varian Cary 5G spectrophotometer. The blank reference was air. Transmittance spectra were recorded in the 200–800 nm wavelength range and the average of three samples was considered.

RESULTS AND DISCUSSION

Preliminary Considerations

PLA has very interesting physicomechanical properties but it also exhibits some limitations when compared to currently engineering or traditional polymers (degradation by hydrolysis, limited mechanical resistance at high temperature, moisture sensitivity, and consequently, degradation during processing, etc.). To overcome some of these drawbacks and to diminish the degradation effects of both moisture and temperature, the addition of CEs into PLA has been recently considered. In this context, it is important to mention that some PLA-Joncryl compositions are already commercialized as masterbatches.^{41,45–47} These CEs are styrene-acrylic multifunctional epoxide oligomers having the general structure shown in Figure 1, while the epoxide coupling reactions with PLA end groups are presented in

Figure 2. More information and details about their features and the mechanisms of reaction with different polymers (including PLA) can be found in the scientific literature and patents, but it is far away from the scope of this article to develop some typical aspects already treated previously.^{37,38,45,48–50}

The CE can be used in a single processing step to substantially increase the molecular weight, mechanical and rheological properties of PLA without the need to fully dry it.^{43,44} However, for PLA blends, it is essential to promote branching while avoiding cross-linking and gel formation. It is also important to know that these CEs are tailored with high or mid epoxy functionality, respectively, to maximize the increase of molecular weights through PLA chains branching for high PLA melt-strength, or to lead to moderate branching and to allow high processing speed.^{43,51} Because the efficiency of epoxide-oligomeric CEs has already been reported for PLA or its blends with other polymers,³⁴ the first objective of this study is to show how much the co-addition of CE and ZnO nanofillers (surface-treated by silane) into PLA affects the molecular, rheological, thermal, and mechanical properties, or is changing the morphology of PLA-ZnO nanocomposites. Accordingly, the comparison of nanocomposites (with and without CE) will be principally concerned hereafter. The second objective is to produce nanocomposites loaded with up to 1% CE exhibiting enhanced performances in the production of films, while maintaining specific end-use properties such as UV screening.

Key Role of CE Addition on Molecular Properties

The modification of molecular weights of PLA matrix in nanocomposites was first studied by SEC analyses. Generally speaking, the degradation of PLA is primarily attributed to hydrolysis triggered by trace amounts of water, zipper-like depolymerization (catalyzed by residual polymerization catalysts), thermo-oxidative reactions, and random main-chain scission during processing, interchain transesterification and depolymerization by back-biting (intramolecular transesterification) resulting in the formation of monomer and cyclic oligomers, residual acidity and presence of different impurities as metals, etc.⁵² However, in the specific case of PLA-ZnO nanocomposites, the degradation of PLA matrix during melt-compounding and processing can be even more advanced due to the presence of Zn ions with effective prodegrading role, especially at high temperature.²⁶ To counterbalance this undesirable effect, the utilization of ZnO nanoparticles surface-treated with silanes such as

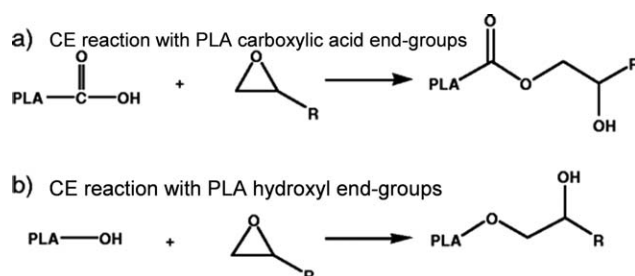


Figure 2. Epoxide coupling reactions with PLA: reaction with (a) carboxylic acid and (b) hydroxyl end-groups (adapted and reprinted with the permission of Springer-Verlag from the reference Corre *et al.*⁴⁷)

Table II. Comparative Molecular Parameters of Neat PLA and PLA–(Surface-Treated) ZnO Nanocomposites (With/Without CE) as Obtained after Melt-Compounding

Sample	M_n (PS)	D (M_w/M_n)
PLA (as received)	133,000	1.9
PLA processed	115,000	2.0
1ZnO	103,200	2.2
1ZnO/0.5J	135,000	2.8
1ZnO/1J	187,100	2.5
3ZnO	99,200	2.1
3ZnO/0.5J	132,800	2.8
3ZnO/1J	202,100	2.4
5ZnO	99,700	2.1
5ZnO/0.5J	103,200	2.9
5ZnO/1J	197,500	2.3

triethoxycaprylsilane is preferred to allow the better preservation of PLA molecular weights with respect to untreated ZnO.²⁷

Table II shows the comparative evaluation of PLA molecular characteristics (M_n and dispersity) of neat PLA (before and after melt-mixing in twin-screw extruder) and of PLA–ZnO nanocomposites (with/without CE). First, for the sake of comparison, it is noteworthy mentioning that under similar conditions of extrusion, the M_n of neat PLA only slightly decreased to about 115,000, which is proving once more PLA sensitivity to temperature, shear, and hydrolysis during melt-processing. In the absence of CE, in the nanocomposites filled with 3–5% ZnO, PLA shows the highest decrease of M_n (~25%), i.e., passing from 133,000 (unprocessed PLA) to about 99,000, after melt-compounding.

On the contrary, a dramatical increase of molecular weights is observed following the addition of CE into the corresponding nanocomposites. By adding 1% CE, the M_n is nearly two times

Table III. Initial Decomposition Temperature ($T_{5\%}$) and Max. Decomposition Temperature (T_d) of PLA–(Surface-Treated) ZnO Nanocomposites (With/Without CE) and of Neat PLA as Determined by TGA (Under Air Flow, 20°C/min)

Sample	Temperature of 5% weight loss, $T_{5\%}$ (°C)	Temperature of max. rate of degradation, T_d (°C)
PLA (as received)	342	381
PLA (processed)	332	379
1ZnO	325	361
1ZnO/0.5J	330	367
1ZnO/1J	336	365
3ZnO	313	354
3ZnO/0.5J	317	360
3ZnO/1J	325	361
5ZnO	307	353
5ZnO/1J	318	357

higher (than those of PLA from nanocomposites without CE), results which clearly attest for CE effectiveness and for the branching of PLA macromolecular chains. Moreover, some larger dispersity and presence of shoulders or multimodal peaks on SEC traces (not shown here) are noticeable. These aspects are usually mentioned for PLA blends with these specific CEs⁴⁰ and are generally attributed to the presence of branched chain populations and to the changes in the polymer topology.⁴¹ As an illustration of CE reactivity, from data shown in Table II, it comes out that addition of 0.5 and 1% CE into PLA filled with 3% ZnO is leading to the increase of M_n , respectively, of about 34 and 104%. This can be a very promising result, in terms of processing ability, stability, and performances.

Thermal Properties

To examine the effects of CE addition on the thermal stability of nanocomposites, TG measurements of PLA–ZnO samples (containing or not CE) have been compared using nonisothermal or isothermal tests. First, it is worth pointing out that the nanofiller has a good thermal stability, thus at the exception of some traces of water, TG curves evidenced only a weight loss of 2.5% up to the temperature of 500°C, which is mainly ascribed to the degradation of alkyl part of triethoxycaprylsilane used for the ZnO surface treatment.

For simplification and easier interpretation, Table III shows the temperature of 5% weight loss ($T_{5\%}$), which is often considered as the initial decomposition temperature, and the temperature corresponding to the maximum rate of thermal degradation (T_d —from d-TG) of nanocomposites with respect to the neat PLA (as received and after processing with twin-screw extruders). From these results, it comes out that in the absence of CE, addition of ZnO nanofiller leads to nanocomposites that show lower values for $T_{5\%}$ and T_d . Moreover, it is observed that the reduction in thermal stability is directly correlated with the percentage of nanofiller, a higher loading with ZnO (e.g., 5%) leading to the most advanced decrease in PLA thermal stability. Again this is not surprising by considering the catalytic role of zinc compounds/products at high temperature in promoting PLA degradation (*vide supra*) leading to the selective formation of lactide and related oligomers.²⁶ On another hand, it is interesting to observe that all nanocomposites containing CE are characterized by better thermal performances (higher $T_{5\%}$ or T_d with respect to the corresponding nanocomposites deprived from any CE). Such improvements, e.g., increasing $T_{5\%}$ by more than 10°C by adding 1% CE, can be readily ascribed to higher PLA molecular weights, and can be considered of real interest in the perspective of nanocomposites application in the production of films and fibers.

In addition, it was also of interest to check the thermal stability of nanocomposites at high temperature and long residence time. To better evidence the CE effect, isothermal TGA was performed at 220 and even 240°C (up to 60 min) for PLA filled with 1 and 5% ZnO.

Figure 3(a,b) shows, respectively, the comparative TG measurements performed under isothermal conditions at 220 and 240°C of PLA filled with 1 and 5% ZnO. A higher thermal stability is observed for the nanocomposites containing CE, while the

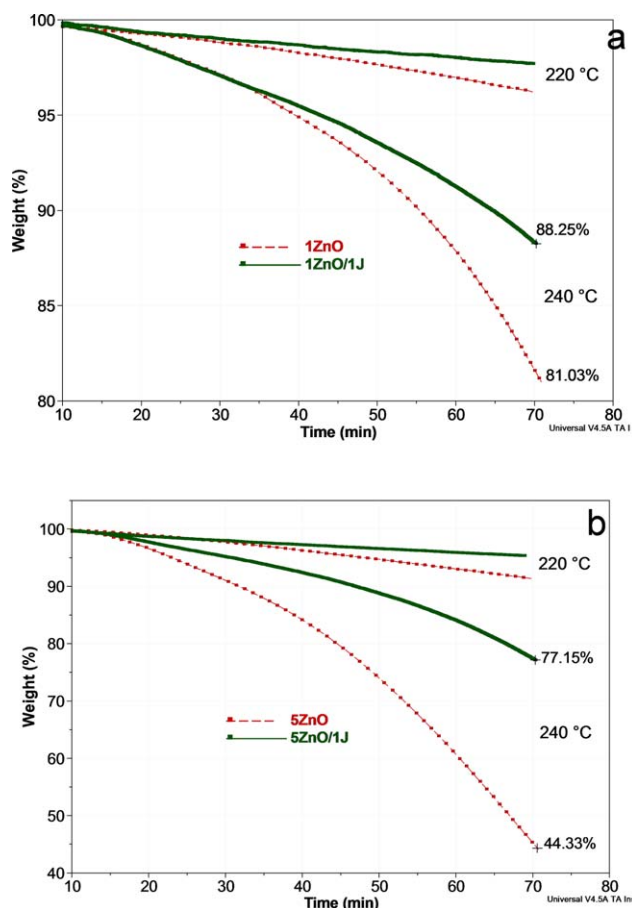


Figure 3. TGA in isothermal conditions (under air) at 220 and 240°C of PLA–ZnO nanocomposites (with/without CE) having different loadings of surface-treated ZnO: (a) 1% and (b) 5%. [Color figure can be viewed in the online issue, which is available at wileyonlinelibrary.com.]

weight loss percentage is related to the nanofiller content. As illustration, the weight loss recorded after 60 min residence time at 220°C for 1ZnO and 5ZnO samples containing 1 and 5% ZnO reached values as high as 3.8 and 8.6%, respectively. Contrarily, the nanocomposites containing 1% CE and similar loadings of ZnO (i.e., 1 and 5%) proved to be more thermally stable, with weight loss limited to only 2.2 and 4.6%, respectively. These differences in favor of PLA nanocomposites containing CE are more impressive at higher temperature (240°C) and high loading (i.e., at 5% ZnO, see Figure 3b).

Regarding the DSC results (data summarized in Table IV), it comes out that there are no significant changes for the values of T_g of PLA which can be connected to the differences of ZnO loading or to the presence or absence of CE. On the other hand, by considering the nanocomposites with similar amount of ZnO, one can observe that the presence of CE (1%) clearly affects the crystallization properties because a delay in PLA crystallization is observed during the second DSC heating (Figure 4). However, these nanocomposites show typically cold crystallization (T_c) at higher temperature, whereas the degree of crystallinity and the T_m are considerably lower than those of the nanocomposites without CE. Interestingly, similar results were reported by Najafi *et al.* for PLA and another CE from the same family.⁵³ The decrease of both degree of crystallinity and rate of crystallization and the increase of T_c were explained by formation of a long-chain branched structure which disrupted the chain packing. Again, the influence of other factors is not totally excluded knowing the difficulty of PLA of high molecular weight to crystallize. Also, it is important to remind that it was previously reported that the silanized ZnO has no significant nucleating effects on PLA.^{27,28}

Rheological Investigations

MFI investigations were first carried out to determine the aptitude of PLA nanocomposites for melt-processing by extrusion. From the values of MFI (Figure 5), it is evident that the addition of increasing amounts of ZnO strongly affects the PLA melt flowing/rheology, a higher fluidity being noticeable for the samples filled with 3 and 5% ZnO in the absence of CE (MFI of, respectively, 13 and 21 g/10 min). This important modification of MFI, observed especially at high percentage of ZnO, is practically associated with the loss in the ability of processing by extrusion due to the higher fluidity and can be mainly explained by the presence of PLA chains of low molecular weight. However, one cannot exclude an additional effect due to presence of alkyl-silane ZnO nanoparticles that can give some lubricating properties. On the other hand, all nanocomposites containing 1% CE show lower MFI (0.5–0.7 g/10 min), which can be interpreted as a better aptitude for processing by extrusion. In addition, the nanocomposites loaded with 1–3% ZnO, but lower amount of CE (0.5%), also remain of interest, the MFI being up to 6 g/10min.

The comparative evolution of complex viscosity of PLA nanocomposites filled with up to 5% ZnO (without/with 1% CE) is plotted as a function of frequency in Figure 6. The complex

Table IV. Comparative DSC Data of Neat PLA and PLA–(Surface-Treated) ZnO Nanocomposites With/Without CE (Second DSC Heating, 10°C/min)

Sample	T_g (°C)	T_c (°C)	ΔH_c (J g ⁻¹)	T_m (°C)	ΔH_m (J g ⁻¹)	χ_c (%)
PLA	63	112	29.4	169	33.5	4.4
1ZnO	63	110	23.7	168	31.9	8.8
1ZnO/1J	63	126	24.2	163	28.2	4.3
3ZnO	63	113	28.9	163; 169	35.1	6.7
3ZnO/1J	63	124	26.1	163	28.2	2.3
5ZnO	63	106	26.3	168	32.5	6.7
5ZnO/1J	63	114	25.5	160; 165	26.0	0.5

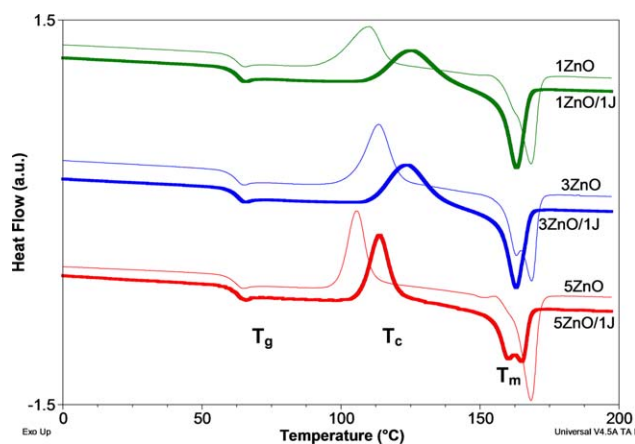


Figure 4. Comparative DSC traces of PLA-(surface-treated) ZnO nanocomposites with and without CE (second DSC heating, 10°C/min). [Color figure can be viewed in the online issue, which is available at wileyonlinelibrary.com.]

viscosity of PLA nanocomposites that do not contain CE is clearly lower than those of nanocomposites containing CE. These results are not surprising by considering the other observations made here about, e.g., the molecular weights and MFI values. However, for both categories of nanocomposites (i.e., with and without CE), the increase in ZnO loading has effect the reduction in viscosity in all frequency range, while a shear-thinning behavior is typically more evident in the case of nanocomposites of higher viscosity (PLA-ZnO/1J samples). On the other hand, by considering the differences in viscosity, lower than 1000 Pa s (PLA-ZnO) and much higher than this value for PLA-ZnO/1J nanocomposites (at frequencies up to about 100 rad/s), it is presumed that different conditions of extrusion must be used for adequate processing. Once more, when the comparative processing ability/stability is considered, PLA-ZnO/1J nanocomposites, due to their higher viscosity, show evident advantages and will offer further flexibility.

According to literature, the rheological characterization of PLA blends containing CEs can reveal the influence of different factors (loading and functionality of CE, effects of chain extension/branching on melt-strength, changes in the PLA rheological behavior linked to the contribution of shear, temperature, residence time, etc.).^{35,36,41} Thus, the studies dealing with the reactions between polyesters (such as PLA) and epoxies

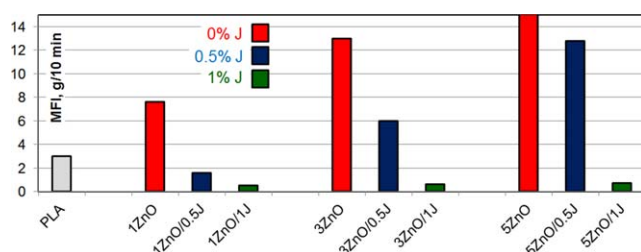


Figure 5. Comparative evaluation of MFI (at 190°C, 2.16 kg) of PLA-(surface-treated) ZnO nanocomposites (with/without CE). [Color figure can be viewed in the online issue, which is available at wileyonlinelibrary.com.]

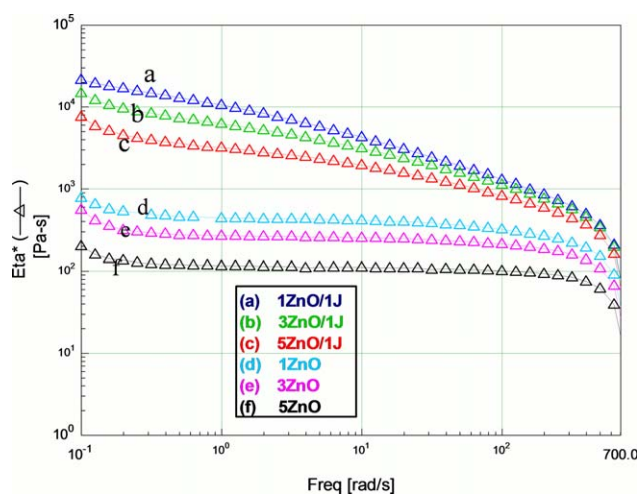


Figure 6. Complex viscosity of PLA-(surface-treated) ZnO nanocomposites (without/with 1% CE) as function of frequency at the temperature of 200°C. [Color figure can be viewed in the online issue, which is available at wileyonlinelibrary.com.]

have considered that under different experimental conditions, a variety of polymer topologies may be obtained, going from linear, branched, and hyperbranched structures to cross-linked structures. Interestingly, for similar PLA and CE grades, but in the absence of ZnO which leads also to the decrease of PLA molecular weights, Cailloux *et al.* have assumed a competition between PLA degradation and chain extension, as well as the evidence of chain branching reactions during processing.⁴¹ For sake of clarity, the specific aspects regarding the rheological characterizations will be developed in a further contribution.

Morphology of PLA-ZnO Nanocomposites Containing CE

It was formerly reported that the surface coating of ZnO by alkyl-silane provides finer distribution and dispersion of the nanoparticles through PLA as matrix.^{27,28}

Figure 7(a-d) shows selected TEM images of PLA-3% ZnO nanocomposites produced in the presence of 0.5 and 1% CE. It is obvious from the TEM images that even by increasing the viscosity of PLA in the molten state due to the addition of CE (see the section entitled “Rheological Investigations”) in the nanocomposites filled with 3% ZnO, the nanoparticles are quite well distributed and dispersed through PLA matrix [Figure 7(a,c)]. Moreover, TEM images performed at higher magnification [Figure 7(b,d)] show the limited presence of some remaining ZnO clusters.

PLA-ZnO Nanocomposites for Films with Specific End-Use Properties

In the second experimental step, selected PLA-ZnO nanocomposites (with/without CE) have been tested by extrusion to produce films. First of all, on one hand, a better processing ability and stability was typically observed in the case of nanocomposites containing 1% CE and this behavior (up to twofold higher torque, evident improvements in melt strength, etc.) was practically ascribed to the higher viscosity of the molten polymer and to the better preservation of PLA molecular weights during extrusion (Table V).

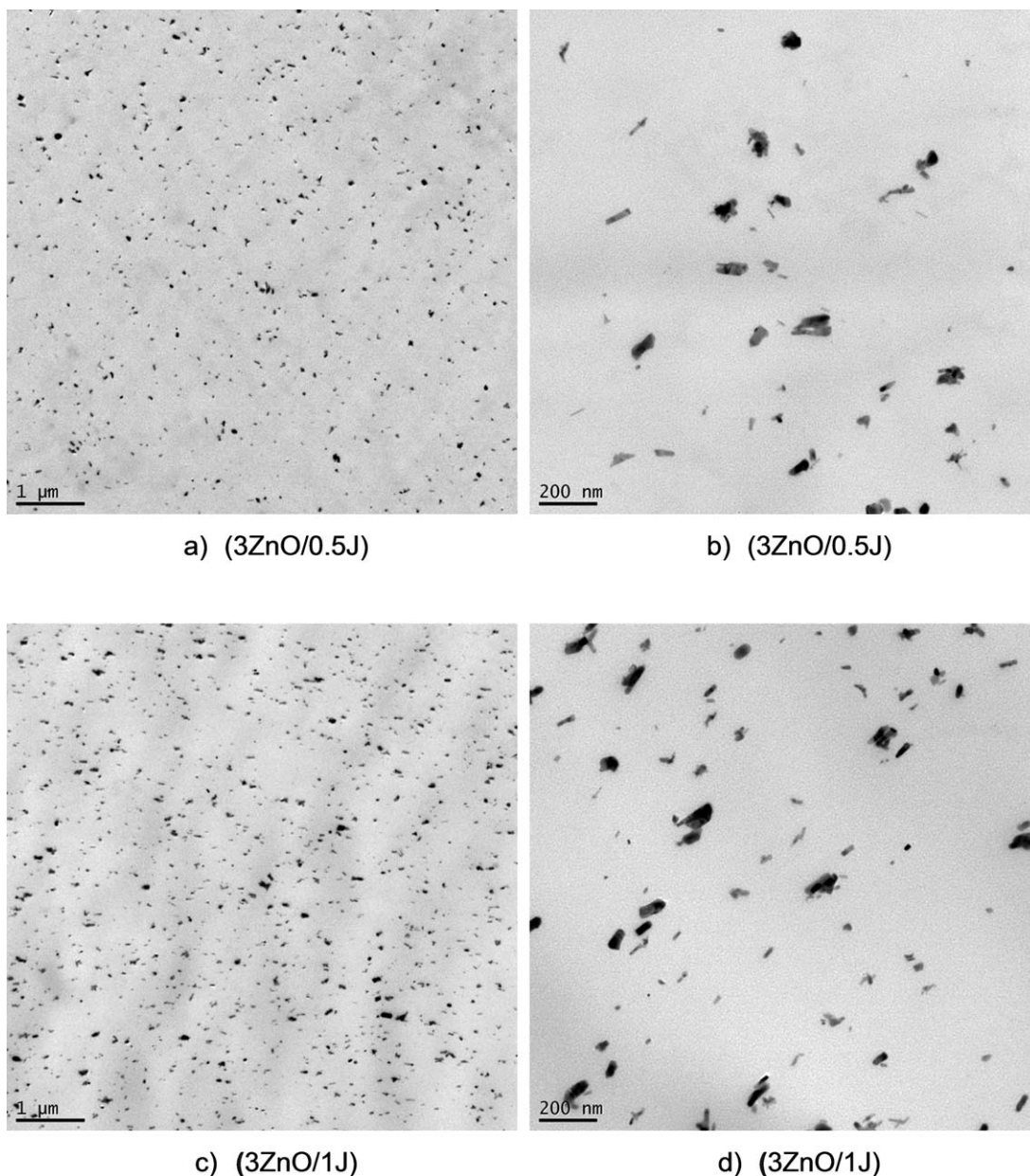


Figure 7. TEM pictures at different magnifications of PLA–3% (surface-treated) ZnO nanocomposites containing (a,b) 0.5% and (c,d) 1% CE.

On the other hand, especially in the case of PLA–5% ZnO nanocomposites without CE (5ZnO sample), it was evident the advanced decrease of melt viscosity (in agreement with MFI values). Furthermore, for PLA-based nanocomposites of high fluidity, i.e., without CE, it was more difficult to control the extrusion process to produce films.

On the contrary, PLA–ZnO/J nanocomposites have shown in all cases improved processing. However, this progress can be of further interest by considering the industrial extrusion process (i.e., low to high residence time and large temperature interval), allowing to obtain extruded products of better quality. Nevertheless, it is considered that the selected CE provides a flexible method for introducing a tunable amount of branching on PLA chains without the evident risk of forming cross-linked

structures. Additionally, the comparative TGA of nanocomposite films proved evident improvements in thermal stability in the favor of PLA–ZnO/1J nanocomposites, i.e., the onset of thermal degradation ($T_{5\%}$) was higher with 10 and even 20°C for loadings of 1 and 5% nanofiller, respectively.

Mechanical parameters were evaluated on dog-bone specimens obtained by cutting from 100- μm -thick films (neat PLA, PLA–ZnO, and PLA–ZnO/1J samples). As shown in Table VI, the increase of ZnO loading up to 5% leads for both families of nanocomposites (having/or not CE) to a slight increase of rigidity (Young's modulus, E) in quite good correlation with the percentage of nanofiller. On the other hand, the rise of ZnO loading leads, more or less, to the reduction of the maximum tensile strength for both types of nanocomposites, i.e., with/

Table V. Comparative Molecular Parameters of PLA–(Surface-Treated) ZnO Nanocomposites (With/Without CE) as Extruded Films

Sample	$M_n(\text{PS})$	$D (M_w/M_n)$
1ZnO	70,000	2.2
1ZnO/0.5J	99,000	3.2
1ZnO/1J	133,000	2.7
3ZnO	55,000	2.1
3ZnO/0.5J	63,000	3.3
3ZnO/1J	98,000	3.1
5ZnO	48,000	2.1
5ZnO/0.5J	54,000	3.5
5ZnO/1J	116,000	3.0

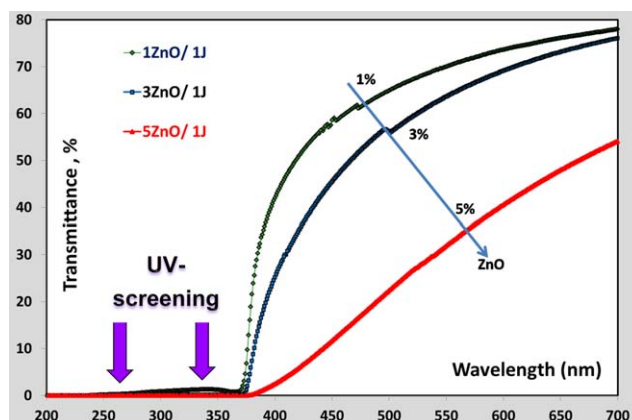
without CE. Furthermore, somewhat unexpected by considering the initial molecular parameters of nanocomposites, tensile stress at both yield (σ_y) and break (σ_b) on the thin films of 100 μm thickness were found slightly higher in the absence of CE. For instance, these differences are ascribed to the low degree of crystallinity of the nanocomposites containing CE, but the influence of other factors cannot be totally excluded. Last, interestingly enough, the PLA–ZnO/J nanocomposite films show in all cases significantly better elongation at yield (ε_y) and break (ε_b) with respect to the nanocomposites without CE.

It is noteworthy reminding that the PLA–ZnO nanocomposites have already been tested in the production of fibers, films, or other materials, showing multifunctional properties (anti-UV, antibacterial, barrier, etc.) which had been proved to be dependent on ZnO loading.^{27,28} The anti-UV and antibacterial properties were confirmed, respectively, at 1 and 3% loading, while additional features (such as self-cleaning) are expected at higher ZnO amount, i.e., at 5% ZnO. Likewise, it is assumed that the co-addition of up to 1% CE and similar ZnO amounts will not negatively affect the specific end-use properties of nanocomposites.

It is also important to point out some key aspects concerning the degradation of these nanocomposites under different conditions of utilization. Using high loadings of nanoparticles, but without a previous treatment, it was reported by Qu Meng *et al.* that ZnO can catalyze rapidly the hydrolytic degradation of PLA at temperatures well below its T_g .⁵⁴ Thus, it was assumed that limiting the decrease of PLA molecular weights

Table VI. Comparative Mechanical Properties of Neat PLA and PLA–(Surface-Treated) ZnO Nanocomposite Films (100 μm Thickness) Having or Not CE (Standard Deviations are Given in Brackets)

Sample	E (MPa)	σ_y (MPa)	σ_b (MPa)	ε_y^* (%)	ε_b^* (%)
neat PLA	3500 (± 150)	44 (± 3)	38 (± 3)	1.5 (± 0.1)	9.8 (± 2.2)
1ZnO	3450 (± 100)	52 (± 2)	45 (± 2)	1.5 (± 0.1)	4.9 (± 1.2)
1ZnO/1J	3150 (± 100)	46 (± 3)	42 (± 3)	2.1 (± 0.5)	12.9 (± 3.1)
3ZnO	3500 (± 100)	46 (± 2)	41 (± 2)	1.5 (± 0.1)	2.6 (± 0.7)
3ZnO/1J	3300 (± 200)	43 (± 5)	39 (± 5)	1.8 (± 0.4)	7.5 (± 2.4)
5ZnO	3850 (± 300)	43 (± 4)	39 (± 4)	1.3 (± 0.1)	1.8 (± 0.2)
5ZnO/1J	4100 (± 250)	36 (± 2)	32 (± 4)	1.5 (± 0.2)	8.9 (± 1.7)

**Figure 8.** UV–vis spectra on selected samples of PLA–(1–5)% ZnO/1J nanocomposite films (thickness of ca 100 μm). [Color figure can be viewed in the online issue, which is available at wileyonlinelibrary.com.]

though the surface treatments of ZnO nanoparticles could be a promising technique leading to nanocomposites with improved resistance to the hydrolytic degradation. In this context, it has recently been reported by us the results of another study concerning the hydrolytic degradation of thin films of PLA–(surface-treated) ZnO nanocomposites in phosphate buffer solution even for more than 10 months.⁵⁵ Following the conclusion of this study, the delayed degradation of nanocomposites with respect to neat PLA was ascribed to a slowdown of the water diffusion into PLA matrix, thanks to significant increase of the crystallinity and especially to the hydrophobic properties of ZnO nanofiller treated with triethoxycaprylylsilane. Additionally, it was examined the effect of light on PLA–(surface-treated) ZnO nanocomposites films produced by extrusion and the attention was focused on the discrimination between the photocatalytic degradation of PLA provoked by ZnO and UV screening effect of ZnO nanoparticles.²⁹ The results indicated that the photocatalytic activity of ZnO nanoparticles induces the oxidation of PLA. Interestingly, because ZnO limits the penetration of light inside the films, this effect mainly concerns only the first microns at the surface of the exposed samples.

Compared to PLA–ZnO nanocomposites, the neat PLA films do not offer any UV protection at wavelength in the range 240–380 nm.²⁷ Figure 8 shows the UV–vis spectra of PLA–ZnO/1J

nanocomposites (films of about 100 μm) at different loadings of nanofiller. From these results, it comes out that addition of 1% ZnO leads to PLA nanocomposites showing almost a perfect UV-shielding effect while maintaining rather a good transmittance in the visible range of the spectra for films containing up to 3% nanofiller (however, a good contact clarity was qualitatively evidenced for films at lower ZnO loading, please consider the Supporting Information, Figure S1(a,b)). It clearly appears that the resulting films are characterized by effective UV protection, whereas the light transmittance in the visible range is only affected by the loading of nanofiller, because an important decrease is seen especially for films loaded with 5% ZnO.

CONCLUSIONS

PLA nanocomposites characterized by multifunctional end-use properties (anti-UV, antibacterial, gas barrier, self-cleaning, etc.) are of high interest as biomaterials for the production of films, fibers, and injection-molded items. Following an original approach, new PLA–ZnO nanocomposites filled with up to 5% nanofiller were produced *via* melt-blending technology and using specifically silane-treated nanoparticles to limit the ZnO degrading effects on polyester matrix.

This study reveals the beneficial effects of a selected CE from the category of epoxy functional styrene-acrylate oligomers on the properties of PLA–ZnO nanocomposites. Indeed, it was possible to melt-compound PLA, ZnO nanofiller, and 0.5 or 1% CE to produce nanocomposites with specific end-use properties. More precisely, by addition of 1% CE, the PLA molecular weights (M_n) were found to increase nearly twofold with respect to those of PLA from nanocomposites without CE. These results attest for the effectiveness of CE in presence of ZnO. Moreover, the samples containing CE were characterized by a higher $T_{5\%}$ (the onset of thermal degradation) while the isothermal tests at high temperature (220 and 240°C) proved a very significant gain in thermal stability at longer residence time. CE addition also plays a key role refining the processability by extrusion of relatively highly filled nanocomposites (3–5% ZnO) to produce films. This is ascribed to the rheological improvements, i.e., better preserving of low MFI, increased viscosity, and melt strength in the molten state. The good dispersion/distribution of ZnO nanoparticles at nanoscale level was evidenced once more by TEM, whereas the tensile tests have shown that the tensile strength and rigidity are mainly determined by the loading of nanofiller. Furthermore, the specific end-use properties following ZnO addition are maintained (e.g., UV protection), whereas additional features (antibacterial, barrier, and self-cleaning, etc.) are expected. Finally, the association of ZnO and CE is regarded as an innovative and promising approach that can pave the way to high-performance products (showing better processing, improved molecular and thermomechanical parameters, multifunctional end-use properties, etc.) and to the larger application of PLA–ZnO nanocomposites.

ACKNOWLEDGMENTS

Authors thank the Wallonia Region, Nord-Pas de Calais Region and European Community for the financial support in the frame of the IINTERREG IV—NANOLAC project. They thank all collaborators from the groups of Prof. Serge Bourbigot (ENSC Lille) and

of Prof. Eric Devaux (ENSAIT Roubaix) for helpful discussions. Authors are grateful to Roelof Van-der-Meer (Joncryl Functional Additives Europe, BASF Nederland B.V.) for supplying Joncryl samples and technical support, to Umicore (Belgium) for ZnO samples and also to Anne-Laure Dechief, Alice Belfiore, and Lisa Dangreau (Materia Nova, Belgium) for assistance in analyses. This work has also been supported by the European Commission and Région Wallonne FEDER program (Materia Nova), Interuniversity Attraction Pole program of the Belgian Federal Science Policy Office (PAI 6/27) and by FNRS-FRFC. J.-M. Raquez is a “FRS-FNRS” Research Associate.

REFERENCES

1. Platt, D. K. *Biodegradable Polymers Market Report*; Smithers Rapra: Shrewsbury: Shropshire, UK, **2006**.
2. Ravenstijn, J. *The State-of-the-Art on Bioplastics: Products, Markets, Trends, and Technologies*; Polymedia Publisher GmbH: Lüdenscheid, Germany, **2010**.
3. Drumright, R. E.; Gruber, P. R.; Henton, D. E. *Adv. Mater.* **2000**, *12*, 1841.
4. Koronis, G.; Silva, A.; Fontul, M. *Compos. Part B* **2013**, *44*, 120.
5. Sinha Ray, S.; Bousmina, M. *Prog. Mater. Sci.* **2005**, *50*, 962.
6. Gupta, A. P.; Kumar, V. *Eur. Polym. J.* **2007**, *43*, 4053.
7. Jamshidian, M.; Tehrani, E. A.; Imran, M.; Jacquot, M.; Desobry, S. *Compr. Rev. Food Sci. F.* **2010**, *9*, 552.
8. Rasal, R. M.; Janorkar, A. V.; Hirt, D. E. *Prog. Polym. Sci.* **2010**, *35*, 338.
9. Murariu, M.; Dubois, P. *JEC Composites Magazine* **2008**, *45*, 66.
10. Lim, L. T.; Auras, R.; Rubino, M. *Prog. Polym. Sci.* **2008**, *33*, 820.
11. Auras, R.; Harte, B.; Selke, S. *Macromol. Biosci.* **2004**, *4*, 835.
12. Carrasco, F.; Pagès, P.; Gámez-Pérez, J.; Santana, O. O.; MasPOCH, M. L. *Polym. Degrad. Stab.* **2010**, *95*, 116.
13. Gupta, B.; Revagade, N.; Hilborn, J. *Prog. Polym. Sci.* **2007**, *32*, 455.
14. Raquez, J.-M.; Habibi, Y.; Murariu, M.; Dubois, P. *Prog. Polym. Sci.* **2013**, *38*, 1504.
15. Fukushima, K.; Murariu, M.; Camino, G.; Dubois, P. *Polym. Degrad. Stab.* **2010**, *95*, 1063.
16. Murariu, M.; Bonnaud, L.; Yoann, P.; Fontaine, G.; Bourbigot, S.; Dubois, P. *Polym. Degrad. Stab.* **2010**, *95*, 374.
17. Murariu, M.; Dechief, A. L.; Bonnaud, L.; Paint, Y.; Gallos, A.; Fontaine, G.; Bourbigot, S.; Dubois, P. *Polym. Degrad. Stab.* **2010**, *95*, 889.
18. Jayaramudu, J.; Das, K.; Sonakshi, M.; Siva Mohan Reddy, G.; Aderibigbe, B.; Sadiku, R.; Sinha Ray, S. *Int. J. Biol. Macromol.* **2014**, *64*, 428.
19. Murariu, M.; Laoutid, F.; Dubois, P.; Fontaine, G.; Bourbigot, S.; Devaux, E.; Campagne, C.; Ferreira, M.; Solarski, S. In *Polymer Green Flame Retardants*;

- Papaspyrides, C. D.; Kiliaris, P., Eds.; Elsevier: Amsterdam, **2014**, p 709.
20. Mai, F.; Habibi, Y.; Raquez, J.-M.; Dubois, P.; Feller, J.-E.; Peijs, T.; Bilotti, E. *Polymer* **2013**, *54*, 6818.
21. Gorrasi, G.; Pantani, R.; Murariu, M.; Dubois, P. *Macromol. Mater. Eng.* **2014**, *299*, 104.
22. Li, Y.-Q.; Fu, S.-Y.; Mai, Y.-W. *Polymer* **2006**, *47*, 2127.
23. Suman, Goyal, D.; Singh, A.; Kumar, R. *Adv. Sci. Lett.* **2014**, *20*, 1321.
24. Nenna, G.; De Girolamo Del Mauro, A.; Massera, E.; Bruno, A.; Fasolino, T.; Minarini, C. *J. Nanomater.* **2012**, *2012*, 7.
25. Kaur, H.; Rathore, A.; Raju, S. *J. Polym. Res.* **2014**, *21*, 1.
26. Abe, H.; Takahashi, N.; Kim, K. J.; Mochizuki, M.; Doi, Y. *Biomacromolecules* **2004**, *5*, 1606.
27. Murariu, M.; Doumbia, A.; Bonnaud, L.; Dechief, A. L.; Paint, Y.; Ferreira, M.; Campagne, C.; Devaux, E.; Dubois, P. *Biomacromolecules* **2011**, *12*, 1762.
28. Pantani, R.; Gorrasi, G.; Vigliotta, G.; Murariu, M.; Dubois, P. *Eur. Polym. J.* **2013**, *49*, 3471.
29. Therias, S.; Larché, J.-F.; Bussière, P.-O.; Gardette, J.-L.; Murariu, M.; Dubois, P. *Biomacromolecules* **2012**, *13*, 3283.
30. Villalobos, M.; Awojulu, A.; Greeley, T.; Turco, G.; Deeter, G. *Energy* **2006**, *31*, 3227.
31. Yang, L.; Chen, X.; Jing, X. *Polym. Degrad. Stab.* **2008**, *93*, 1923.
32. Cicero, J. A.; Dorgan, J. R.; Dec, S. F.; Knauss, D. M. *Polym. Degrad. Stab.* **2002**, *78*, 95.
33. Fan, W.; Zhao, Y.; Zhang, A.; Liu, Y.; Cao, Y.; Chen, J. *J. Appl. Polym. Sci.* **2014**, *132*, 41561, doi: 10.1002/app.41561.
34. Dong, W.; Zou, B.; Yan, Y.; Ma, P.; Chen, M. *Int. J. Mol. Sci.* **2013**, *14*, 20189.
35. Meng, Q.; Heuzey, M.-C.; Carreau, P. J. *Polym. Degrad. Stab.* **2012**, *97*, 2010.
36. Meng, Q. K.; Heuzey, M. C.; Carreau, P. J. *Int. Polym. Proc.* **2012**, *27*, 505.
37. Najafi, N.; Heuzey, M. C.; Carreau, P. J. *Compos. Sci. Technol.* **2012**, *72*, 608.
38. Najafi, N.; Heuzey, M. C.; Carreau, P. J.; Wood-Adams, P. M. *Polym. Degrad. Stab.* **2012**, *97*, 554.
39. Nofar, M.; Zhu, W.; Park, C. B.; Randall, J. *Ind. Eng. Chem. Res.* **2011**, *50*, 13789.
40. Randall, J. R.; Cink, K.; Smith, J. C. Branching Polylactide by Reacting OH or COOH Polylactide with Epoxide Acrylate (co)Polymer. US7566753 B2, Google Patents: **2009**.
41. Cailloux, J.; Santana, O. O.; Franco-Urquiza, E.; Bou, J. J.; Carrasco, F.; Gamez-Perez, J.; MasPOCH, M. L. *EXPRESS Polym. Lett.* **2013**, *7*, 304.
42. Zhang, Y.; Yuan, X.; Liu, Q.; Hrymak, A. J. *Polym. Environ.* **2012**, *20*, 315.
43. Anon. Upgrade your recycled plastic! Plastic additives – the JONCRYL selection guide, BASF (<http://twinstar-corp.com/wp-content/uploads/2012/05/basf-additives/ADJRBA001%20BASF%20Joncryl.pdf>, accessed December 26, 2014).
44. Anon. JONCRYL ADR-4300 (technical sheet) - Polymeric chain extender for condensation thermoplastics, BASF, 17 Aug **2006**.
45. Jaszkiwicz, A.; Bledzki, A. K.; Duda, A.; Galeski, A.; Franciszcak, P. *Macromol. Mater. Eng.* **2014**, *299*, 307.
46. Jaszkiwicz, A.; Bledzki, A. K.; van der Meer, R.; Franciszcak, P.; Meljon, A. *Polym. Bull.* **2014**, *71*, 1675.
47. Corre, Y.-M.; Duchet, J.; Reignier, J.; Maazouz, A. *Rheol. Acta* **2011**, *50*, 613.
48. Blasius, W. G.; Deeter, G.; Villalobos, M. Oligomeric chain extenders for processing, post-processing and recycling of condensation polymers, synthesis, compositions and applications. WO2003066704 A1, Google Patents (**2003**).
49. Al-Itry, R.; Lamnawar, K.; Maazouz, A. *Polym. Degrad. Stab.* **2012**, *97*, 1898.
50. Ludwiczak, J.; Kozłowski, M. *J. Polym. Environ.* **2015**, *23*, 137.
51. Frenz, V.; Meer, R. v. d.; Villalobos, M.; Awojulu, A. Polymeric Chain Extenders and Biopolymers; Global Plastics Environmental Conference (GPEC): Orlando, FL, March 11–12, **2008**.
52. Madhavan Nampoothiri, K.; Nair, N. R.; John, R. P. *Biore-sour. Technol.* **2010**, *101*, 8493.
53. Najafi, N.; Heuzey, M. C.; Carreau, P. J. *Polym. Eng. Sci.* **2013**, *53*, 1053.
54. Qu, M.; Tu, H.; Amarante, M.; Song, Y.-Q.; Zhu, S. S. *J. Appl. Polym. Sci.* **2014**, *131*, 40287, doi: 10.1002/app.40287.
55. Benali, S.; Aouadi, S.; Dechief, A.-L.; Murariu, M.; Dubois, P. *Nanocomposites* **2015**, *1*, 51.